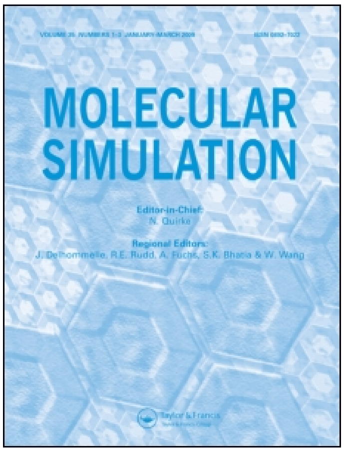

Molecular Simulation
Publication details, including instructions for authors and subscription information:
http://www.informaworld.com/smpp/title~content=t713644482

Study of ZrO_2 phase structure and electronic properties

Fan Qunbo[a]; Wang Fuchi[a]; Zhang Huiling[a]; Zhang Feng[a]
[a] School of Materials Science and Engineering, Beijing Institute of Technology, Beijing, People's Republic of China

To cite this Article Qunbo, Fan , Fuchi, Wang , Huiling, Zhang and Feng, Zhang(2008) 'Study of ZrO_2 phase structure and electronic properties', Molecular Simulation, 34: 10, 1099 — 1103

To link to this Article: DOI: 10.1080/08927020802101759

URL: http://dx.doi.org/10.1080/08927020802101759

Molecular Simulation
Vol. 34, Nos. 10–15, September–December 2008, 1099–1103

Study of ZrO_2 phase structure and electronic properties

Fan Qunbo*, Wang Fuchi, Zhang Huiling and Zhang Feng

School of Materials Science and Engineering, Beijing Institute of Technology, Beijing 100081, People's Republic of China

(*Received 19 December 2007; final version received 27 March 2008*)

The phase structure and electronic properties of c-ZrO_2, t-ZrO_2 and m-ZrO_2 are calculated and compared using density functional theory. By calculating the energies for different lattice constants, the crystal structures of the three zirconia polymorphs are optimised. The calculation results are in good agreement with related experimental data and the cohesive energies do reflect the relative phase stability of the three zirconia polymorphs. The valence electronic density of states and the charge distributions on some typical planes are presented and discussed to investigate the valence electronic structure, the special electronic properties, and the Zr—O bond strength. The calculation results in this paper would be helpful to further predict the zirconia phase transition and some basic physical properties.

Keywords: density functional theory; zirconia; phase structure; charge distribution

1. Introduction

Due to their prominent physical and chemical properties, ZrO_2 ceramic materials have been widely used in modern engineering and industry fields, such as fuel cells [1], thermal barrier coatings [2], refractory materials [3], catalysts [4] and so on. It is well known, however, that at ambient pressure ZrO_2 itself is not stable, which has three polymorphic phases: monoclinic (m-ZrO_2, p21/c space group), tetragonal (t-ZrO_2, p42/nmc space group) and cubic (c-ZrO_2, fm3m space group), as illustrated in Figure 1. To better understand and control ZrO_2's properties in practical applications, it is necessary to investigate its phase structures and corresponding charge characteristics, so as to reveal the inner mechanism of the relative stability of these three polymorphic phases.

Up to the present time, density functional theory (DFT) [5] has become one of the most important and valid method to investigate the charge distribution of crystals, and investigate the relationship between micro and macro properties in ground state, especially in quantum chemistry calculation of multi-particle systems. The most outstanding advantage for DFT is that all the calculations are performed without any input from experiment. Jomard [6] calculated the phase stability of different ZrO_2 polymorphs in the framework of DFT, and revealed the tendency of t–c phase transition. Kuwabara [7] successfully computed the Helmholtz free energies of t- and m-ZrO_2, indicating that t-ZrO_2 become more stable than m-ZrO_2 at temperatures higher than 1350 K, and found that vibrational entropy of Zr and O ions is attributed to the stabilisation of t-ZrO_2 at elevated temperatures. The relationship between phase structures and charge characteristics, however, still needs further studies.

Within the framework of DFT, we use the computer code CASTEP [8] to study ZrO_2 crystal structures, cohesive energies, density of states (DOS) of valence electrons, as well as spatial distribution of charges, so as to investigate the underlying relationship between the ZrO_2 crystal structures and charge characteristics.

2. Computation details

All the calculations in this paper are done for the ground state of ZrO_2 crystal structures, and exchange and correlation functional is given by the generalised gradient approximation as proposed by Wang and Perdew [9]. The atomic reference configurations are $4d^25s^2$ for Zr and $2s^22p^4$ for O. The k-point meshes of Brillouin zone sampling in primitive cells, based on the Monkhorst–Pack scheme [10], are $4 \times 4 \times 4$ for c-ZrO_2 (10 irreducible points), $5 \times 5 \times 3$ t-ZrO_2 (12 irreducible points) and $3 \times 3 \times 3$ for m-ZrO_2 (10 irreducible points), in order to obtain energy convergence $\leq 2 \times 10^{-5}$ eV/atom.

As illustrated in Figure 2, input the initial charge density and wave function of crystal structures, then adjust the crystal structure to get new charge density and solve the corresponding energy and force, until both the energy and the force meet the convergence criterion. Finally, the DOS of valence electrons and charge distribution in space are output based on the optimised crystal structures.

---

*Corresponding author. Email: fanqunbo@bit.edu.cn

ISSN 0892-7022 print/ISSN 1029-0435 online

DOI: 10.1080/08927020802101759
http://www.informaworld.com

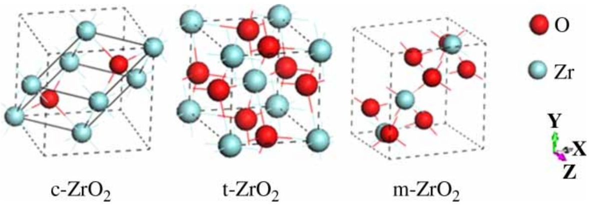

Figure 1. Three polymorphic phases of ZrO_2.

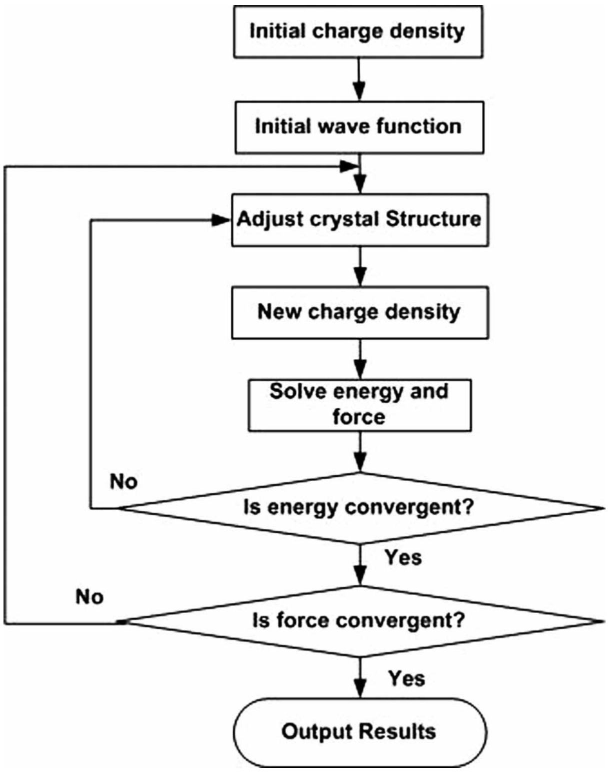

Figure 2. Flow chart of DFT calculation scheme.

3. Results and discussion

3.1 Phase structure and stability

As shown in Figure 1, at the atomic scale, the 8-coordinated zirconium ions form a face-centred cubic lattice and each oxygen ion is located in a 4-coordinated zirconium tetrahedron; t-ZrO_2 is in p42/nmc space group, which can be derived by stretching the cubic one along [001] directions; m-ZrO_2 is in p21/c space group, which can be described as a distorted fluorite structure with the Zr atoms in seven-fold coordinations sites. In addition, there are two oxygen sites in the m-ZrO_2 lattice: O_I and O_{II}. Table 1 lists the internal structural parameters of Zr, O atoms for three ZrO_2 polymorphs. It can be seen that the calculation results agree very well with experimental observations.

As shown in Table 2, the calculated theoretical lattice components for three ZrO_2 polymorphs are compared with previous calculation results and experimental data. It can be seen that both the previous calculation results and the experimental data validate the reliability of the present work. Based on the basic geometry parameters of crystal structures in Tables 1 and 2, the cohesive energies of three ZrO_2 polymorphs are calculated, which is dependent on the lattice constants, and the theoretical cohesive energy corresponds to the minimum value.

Table 3 lists the cohesive energies for the geometry-optimised c-ZrO_2, t-ZrO_2 and m-ZrO_2, with the value of −29.73, −29.81 and 29.93 eV, respectively, which are compared with calculation results reported by other literatures [3,4]. Though the results are somewhat different due to different predefined calculation parameters, such as pseudopotentials, exchange correlation functionals, k-point meshes, a definite relationship can be found: $E_{\text{c-ZrO}_2} > E_{\text{t-ZrO}_2} > E_{\text{m-ZrO}_2}$. Such relationship is consistent with the fact that m-ZrO_2 is the most stable phase under ground state.

3.2 Charge characteristics

3.2.1 Density of states (DOS)

Once the crystal structure is determined, the corresponding valence DOS of the structure can be further determined. Figures 3–5 show the total DOS (TDOS) for c-ZrO_2, t-ZrO_2 and m-ZrO_2, as well as the partial DOS (PDOS) of Zr and O atoms. Since there are two oxygen sites in the

Table 1. Calculated internal structural parameters of ZrO_2 polymorphs in comparison with experimental data.

		Calculations			Experiments [11–13]		
Atom type	Wyckoff notation	*x*	*y*	*z*	*x*	*y*	*z*
c-ZrO_2 (fm3-m)							
Zr	4a	0	0	0	0	0	0
O	8c	0.25	0.25	0.25	0.25	0.25	0.25
t-ZrO_2 (p42/nmc)							
Zr	2a	0	0	0	0	0	0
O	4d	0	0.5	0.1985	0	0.5	0.1980
m-ZrO_2 (p21/c)							
Zr	4e	0.2728	0.0337	0.2088	0.2744	0.0394	0.2084
O_I	4e	0.0733	0.3133	0.3046	0.0614	0.3263	0.3404
O_{II}	4e	0.4619	0.7882	0.4362	0.4495	0.7575	0.4757

Table 2. Theoretical lattice constants obtained for three ZrO_2 polymorphs, compared with previous calculations and experiments.

		This work	Calculations [7]	Calculations [14]	Experiments [15]
c-ZrO_2	a (Å)	5.092	5.145	5.0371	5.108
t-ZrO_2	a (Å)	3.642	3.642	3.5567	3.591
	c (Å)	5.275	5.295	5.1044	5.169
m-ZrO_2	a (Å)	5.158	5.211	5.1083	5.1505
	b (Å)	5.230	5.286	5.1695	5.2116
	c (Å)	5.340	5.388	5.2717	5.3173
	β (°)	99.56	99.59	99.21	99.23

Table 3. Cohesive energies for different ZrO_2 polymorphs.

	This work (eV)	Computation results [7]	Computation results [6]
c-ZrO_2	−29.73	−28.413	−26.18
t-ZrO_2	−29.81	−28.503	−26.20
m-ZrO_2	−29.93	−28.612	−26.18

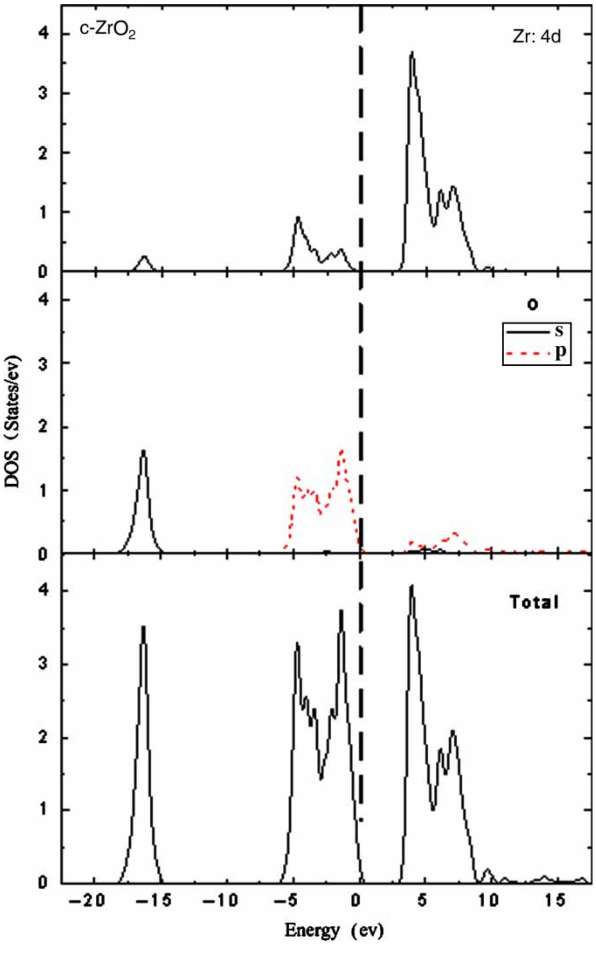

Figure 3. DOS of c-ZrO_2.

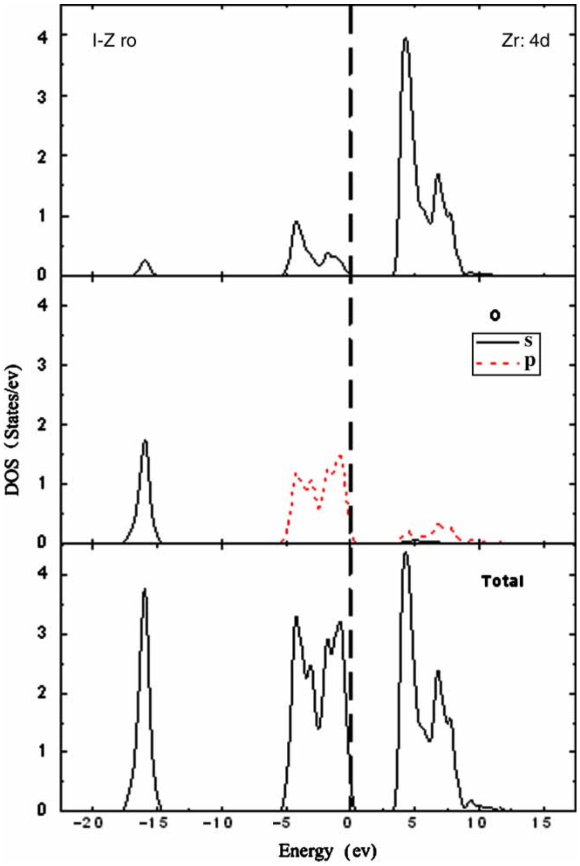

Figure 4. DOS of t-ZrO_2.

m-ZrO_2, we present the corresponding PDOS in Figure 5. Here, Fermi level is at the value of 0 eV for all DOS.

It can be readily seen that these three phases have rather similar DOS features. The bands, spanning between − 18 and − 14 eV are mostly due to O2s orbital. The bands in the energy range from − 5 to − 0 eV, are mainly O2p in character, and partial Zr4d orbital also occupy the same range, indicating a strong Zr—O covalence interaction. The band gap for c-ZrO_2, t-ZrO_2 and m-ZrO_2 is 2.40, 3.17 and 2.98 eV, respectively, reflecting an insulating feature for ZrO_2 as observed experimentally.

3.2.2 Charge densities

To compare the charge distribution characteristics for three ZrO_2 polymorphs, the charge distribution on a typical plane is presented in Figures 6–8, respectively. Figure 6 shows the charge distribution on a typical c-ZrO_2 plane with miller index (1 1 −2) and across the point (2.53, 2.53, 2.53); Figure 7 shows the charge distribution on a typical t-ZrO_2 plane with miller indices (0 1 0) and across the point (1.82, 1.82, 2.64); and Figure 8 shows the

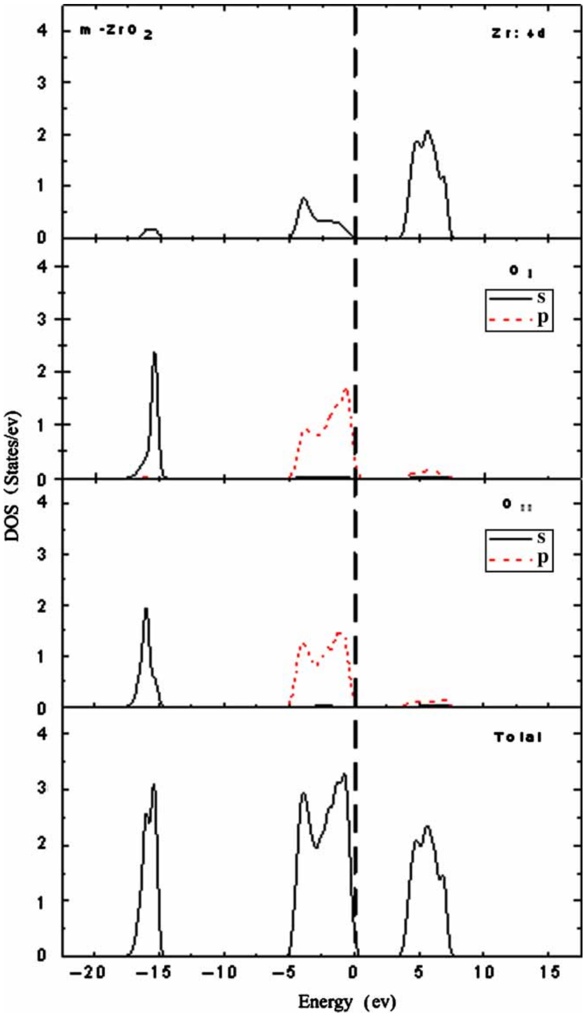

Figure 5. DOS of m-ZrO_2.

charge distribution on a typical m-ZrO_2 plane with miller indices (-0.68 0.68 -0.27) and across the point (2.48, 2.56, 2.20). As shown in these figures, the maximum charge density for c-ZrO_2, t-ZrO_2 and m-ZrO_2 is 5.098, 7.234 and 7.261 electrons/Å^3, respectively, which is agreement with phase stability tendency at ground state. Namely, the larger the maximum charge density is, the stronger the bonding strength is, and the more stable the phase is. In addition, high-density charge exists primarily between Zr and O atoms, also reflecting a strong Zr—O covalence interaction as illustrated in Section 3.2.1.

4. Conclusions

Based on DFT, the crystal and electronic structures of c-ZrO_2, t-ZrO_2 and m-ZrO_2 are studied. Geometry optimisation for three ZrO_2 polymorphs at ground state is conducted, and the cohesive energies account for the related phase stability; DOS and PDOS of three ZrO_2 polymorphs are calculated, indicating a strong Zr—O covalence interaction, which is further validated by calculating the charge distribution on typical ZrO_2 crystal planes. It is found that the larger the maximum charge density is, the stronger the bonding strength is, and the more stable the phase is. The relationship between the phase structures and electronic properties provides an additional way to further investigate the micro phase transition process of ZrO_2, as well as some basic physical properties.

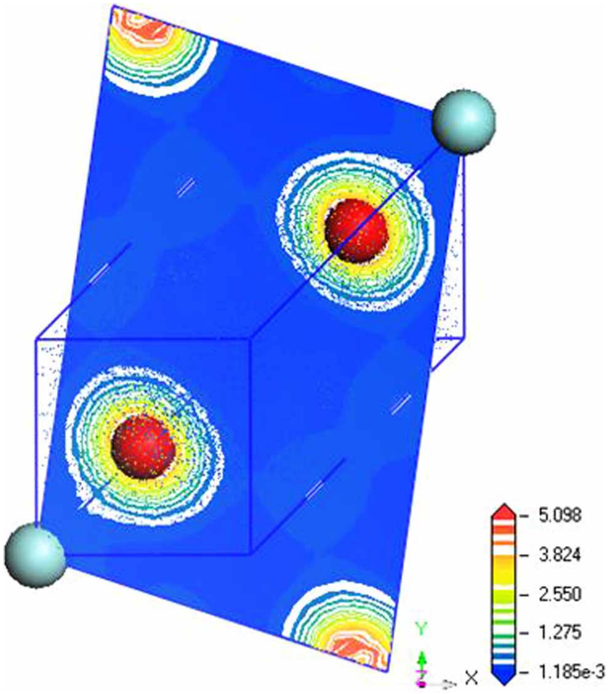

Figure 6. Charge distribution on a typical plane of c-ZrO_2.

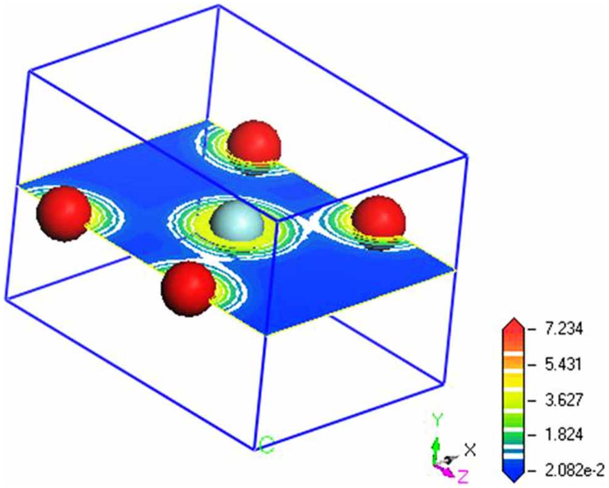

Figure 7. Charge distribution on a typical plane of t-ZrO_2.

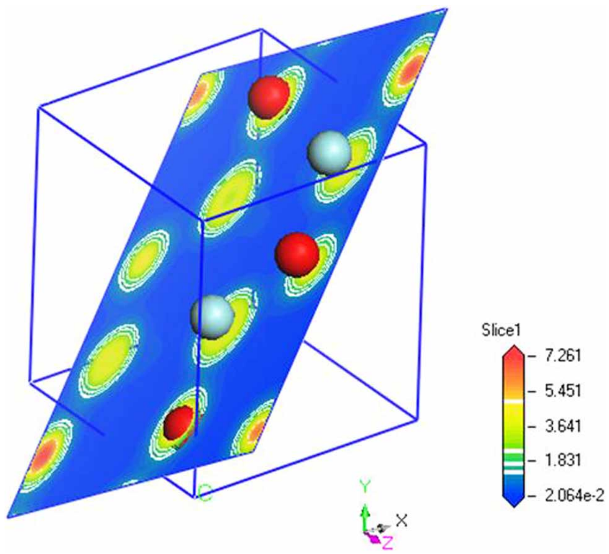

Figure 8. Charge distribution on a typical plane of m-ZrO_2.

Acknowledgements

Support in part by the Commission of Science Technology and Industry for National Defence under grant number 9140A12020306BQ01 and the Excellent Young Teacher Foundation of Beijing Institute of Technology under Contract 1040012040101 is acknowledged.

References

[1] H.J. Cho and G.M. Choi, *Effect of milling methods on performance of Ni* − Y_2O_3*-stabilized* ZrO_2 *anode for solid oxide fuel cell*, J. Power Sources 176(1) (2008), pp. 96–101.

[2] P.C. Tsai, J.H. Lee, and C.L. Chang, *Improving the erosion resistance of plasma-sprayed zirconia thermal barrier coatings by laser glazing*, Surf. Coat. Technol. 202(4–7) (2007), pp. 719–724.

[3] E.Y. Fogaing, M. Huger, and C. Gault, *Elastic properties and microstructure: study of two fused cast refractory materials*, J. Eur. Ceram. Soc. 27(2–3) (2007), pp. 1843–1848.

[4] G. Jin, G. Lu, Y. Guo, Y. Guo, J. Wang, W. Kong, and X. Liu, *Effect of preparation condition on performance of* $Ag - MoO_3/ZrO_2$ *catalyst for direct epoxidation of propylene by molecular oxygen*, J. Mol. Catal. A: Chem. 232(1–2) (2005), pp. 165–172.

[5] P. Hohenberg and W. Kohn, *Inhomogeneous electron gas*, Phys. Rev. 136(3) (1964), pp. B864–B871.

[6] G. Jomard, T. Petit, A. Pasturel, L. Magaud, G. Kresse, and J. Hafner, *First-principles calculations to describe zirconia pseudo-polymorphs*, Phys. Rev. B 59(6) (1999), pp. 4044–4052.

[7] A. Kuwabara, T. Tohei, T. Yamamoto, and I. Tanaka, Ab initio *lattice dynamics and phase transformations of* ZrO_2, Phys. Rev. B 71 (2005), 064301.

[8] M.D. Segall, P. Lindan, M.J. Probert, C.J. Pickard, P.J. Hasnip, S.J. Clark, and M.C. Payne, *First-principles simulation: ideas, illustrations and the CASTEP code*, J. Phys. Condens. Matter 14(11) (2002), pp. 2717–2744.

[9] Y. Wang and J.P. Perdew, *Correlation hole of the spin-polarized electron gas, with exact small-wave-vector and high-density scaling*, Phys. Rev. B 44(24) (1991), pp. 13298–13307.

[10] H.J. Monkhorst and J.D. Pack, *Special points for Brillouin-zone integrations*, Phys. Rev. B 13 (1976), pp. 5188–5192.

[11] D.N. Wang, Y.Q. Guo, K.M. Liang, and K. Tao, *Crystal structure of zirconia by Rietveld refinement*, Sci. China, Ser. A 42(1) (1999), pp. 80–86.

[12] N. Igawa and Y. Ishii, *Crystal structure of metastable tetragonal zirconia up to 1473 K*, J. Am. Ceram. Soc. 84(5) (2001), pp. 1169–1171.

[13] F.J. Torres, J.M. Amigo, and J. Alarcon, *X-ray powder diffraction study of monoclinic* V^{4+}*-*ZrO_2 *solid solutions obtained from gels*, J. Solid State Chem. 173 (2003), pp. 40–44.

[14] X. Zhao and D. Vanderbilt, *Phonons and lattice dielectric properties of zirconia*, Phys. Rev. B 65 (2002), 075105.

[15] N. Igawa, Y. Ishii, T. Nagasaki, Y. Morii, S. Funahashi, and H. Ohno, *Crystal structure of metastable tetragonal zirconia by neutron powder diffraction study*, J. Am. Ceram. Soc. 76 (1993), pp. 2673–2676.